

Correlation of electronic structure and ordered charge and orbital patterns for single-layered manganites in a wide hole-doping range ($0 \leq x \leq 1$)

Y. S. Lee,^{1,2} T. Arima,^{1,3} S. Onoda,¹ Y. Okimoto,⁴ Y. Tokunaga,¹ R. Mathieu,¹ X. Z. Yu,¹ J. P. He,¹ Y. Kaneko,¹ Y. Matsui,⁵ N. Nagaosa,^{4,6} and Y. Tokura^{1,4,6}

¹*Spin Superstructure Project and Multiferroics Project, ERATO, Japan Science and Technology Agency, Tsukuba 305-8562, Japan*

²*Department of Physics, Soongsil University, Seoul 156-743, Korea*

³*Institute of Multidisciplinary Research for Advanced Materials, Tohoku University, Sendai 980-8577, Japan*

⁴*Correlated Electron Research Center (CERC), National Institute of Advanced Industrial Science and Technology (AIST), AIST Tsukuba Central 4, Tsukuba 305-8562, Japan*

⁵*Advanced Materials Laboratory, National Institute for Materials Science (NIMS), Tsukuba 305-0044, Japan*

⁶*Department of Applied Physics, University of Tokyo, Tokyo 113-8656, Japan*

(Received 29 January 2007; published 6 April 2007)

We investigated the doping-dependent evolution of the charge-orbital ordering (CO-OO) phase using optical spectroscopy of a series of single-layer manganites, $\text{La}_{1-x}\text{Sr}_{1+x}\text{MnO}_4$ ($x=0$ and 1) and $\text{Pr}_{1-x}\text{Ca}_{1+x}\text{MnO}_4$ ($0.3 \leq x \leq 0.7$). We found that the electronic response of the CO-OO phase changes asymmetrically with respect to the addition or removal of e_g electrons from $x=1/2$. Especially, low-energy optical spectra depend strongly on the modulation vector of striped phase in a higher doping region ($x \geq 1/2$). This finding highlights the role of the nanoscale structure of e_g ordering in the electronic property of the striped phase in the layered manganite.

DOI: [10.1103/PhysRevB.75.144407](https://doi.org/10.1103/PhysRevB.75.144407)

PACS number(s): 75.47.Gk, 75.30.Et, 78.40.Ha

I. INTRODUCTION

The physics of doped Mott insulators is at the focus of current research on strongly correlated electronic system because of a variety of intriguing ground states that originate from strong correlations among the doped holes.¹ One of the interesting examples is the one-dimensional (1D) charge-spin superstructure, referred to as stripe. The charge-spin striped phase has been observed with a strong doping concentration dependence in some two-dimensional (2D) Cu and Ni oxides. On the other hand, in a situation where the orbital degree of freedom is active, the striped pattern is even more peculiar, which is the case of charge-orbital stripe observed for some Mn oxides in close relation to the magnetic correlation.²⁻⁵ For example, at half doping ($x=1/2$), the zigzag chain-type e_g orbital arrangement along the direction perpendicular to the charge stripe is formed below the charge-orbital ordering (CO-OO) transition temperature $T_{\text{CO-OO}}$ and drives the CE-type magnetic order below Néel temperature T_N ($\leq T_{\text{CO-OO}}$): the ferromagnetic (FM) spin ordering along the zigzag chain and the antiferromagnetic (AFM) coupling between neighboring chains. These peculiar properties of the charge-orbital stripe imply that the manganite may provide an important laboratory to investigate the role of the orbital degree of freedom in determining the electronic property of the striped phase.

In pseudocubic perovskite (113) manganites, the competition between CO-OO and FM correlations leads to a complex nature of phase diagram with a metal-insulator transition.⁵ Moreover, various ordering types are observed with doping. For example, the ground states of $\text{Nd}_{1-x}\text{Sr}_x\text{MnO}_3$ are FM for $x=0.4$, CO-OO and CE-type AFM for $x=0.5$, A type for $x=0.55$, and C type for $x=0.65$.^{6,7} In a single-layer (214) structure, on the other hand, the low-temperature FM correlation is almost suppressed⁸ and insulating phases are dominant in an entire

doping range. Indeed, the CO-OO phase of the $\text{Pr}_{1-x}\text{Ca}_{1+x}\text{MnO}_4$ (PCMO) series is robust in a relatively wide doping range of $0.35 \leq x \leq 0.75$.^{9,10} In this situation, it is feasible to access the generic doping-dependent evolution of the CO-OO state without any disturbance of FM correlation. Notably, the phase diagram for the CO-OO phase in the 214 structure shows an asymmetric behavior around $x=1/2$: the CO-OO correlation is weakened for $x \leq 1/2$, whereas the modulation period of the charge-orbital stripe changes systematically with doping for $x \geq 1/2$.^{8,9,11,12} Most likely this asymmetric doping dependence is attributed to a peculiar e_g orbital correlation. To elucidate this, optical spectroscopy on the electronic structure of the insulating CO-OO state will be useful. In this paper, we report on the in-plane optical study of the $\text{Pr}_{1-x}\text{Ca}_{1+x}\text{MnO}_4$ series where the CO-OO state is robust in a relatively wide doping range of $0.35 \leq x \leq 0.75$.^{9,10} In an effort to reveal the electronic structure in the layered manganites including the end member compounds, it is found that the low-energy absorption formed by introducing holes depends strongly on the CO-OO pattern as well as x . The significant change in the spectral shape with the stripe periodicity is compared with a theoretical calculation.

II. EXPERIMENT

$\text{Pr}_{1-x}\text{Ca}_{1+x}\text{MnO}_4$ ($0.3 \leq x \leq 0.7$), LaSrMnO_4 ($x=0$), and Sr_2MnO_4 ($x=1$) single crystals were grown by the floating-zone method.¹¹ To characterize the CO-OO phase of the PCMO series, we performed measurements of dc resistivity, magnetization, and electron diffraction pattern measurements. T -dependent reflectivity spectra $R(\omega)$ at nearly normal incidence were measured for the Mn-O plane (ab plane) at photon energies from 0.06 to 5 eV with T variation from 10 to 400 K and connected smoothly to room-temperature $R(\omega)$ above 5–40 eV, which was measured with synchrotron

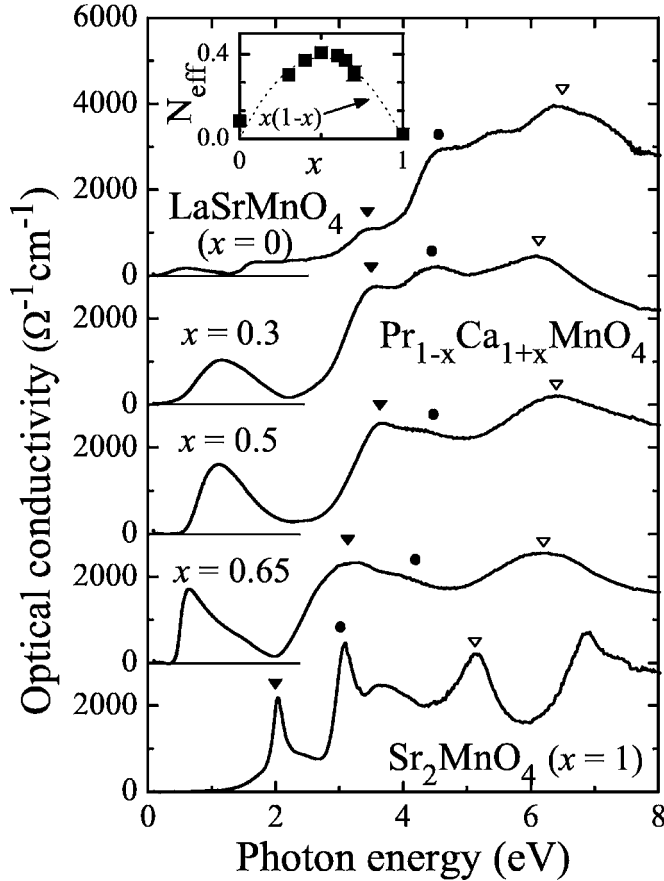


FIG. 1. Optical conductivity spectra for LaSrMnO_4 , PCMO with $x=0.3, 0.5, \text{ and } 0.65$, and Sr_2MnO_4 . The inset displays the x dependence of N_{eff} ($\omega_c=2$ eV).

radiation at UV-SOR, Institute for Molecular Science, Japan. Optical conductivity spectra $\sigma(\omega)$ were obtained from the measured $R(\omega)$ using the Kramers-Kronig transformation.

III. RESULTS AND DISCUSSIONS

A. Overall spectra of optical conductivity of single-layer manganites for $0 \leq x \leq 1$

We first discuss the overall electronic structure of the 214 manganite in terms of the optical conductivity analysis. Figure 1 shows the $\sigma(\omega)$ at 10 K for LaSrMnO_4 ($x=0$),¹³ $\text{Pr}_{1-x}\text{Ca}_{1+x}\text{MnO}_4$ (PCMO) with $x=0.3, 0.5, \text{ and } 0.65$, and Sr_2MnO_4 ($x=0$).¹⁴ Distinct absorptions observed in $\sigma(\omega)$ are categorized into two classes: $d-d$ transitions between e_g orbitals below 2 eV and charge transfer (CT) excitations from O $2p$ to Mn $3d$ bands above 2 eV. First, we focus on the latter. Three distinct absorption peaks above 2 eV are commonly observed for all the samples, marked by the solid triangles, the circles, and the open triangles from the lowest energy.¹⁵ Taking into account the multiplet splitting of the final state, we assign these absorptions to transitions from the O $2p$ band to the Mn $e_g \uparrow$ (spin up), $t_{2g} \downarrow$ (spin down), and $e_g \downarrow$ bands, with the common $t_{2g}^3 \uparrow$ configuration. The energy differences between the Mn $t_{2g} \downarrow$ and $e_g \downarrow$ states and between the Mn $e_g \uparrow$ and $e_g \downarrow$ states correspond to the crystal-field splitting

and Hund's rule coupling energy, and are therefore estimated to be ~ 2 and ~ 3 eV, respectively, from the measured $\sigma(\omega)$.

A conspicuous feature in $\sigma(\omega)$ below 2 eV is a strong doping dependence of the spectral weight. In a Mott insulator LaSrMnO_4 where all Mn ions have $3+$ valence, a weak absorption near 1.5 eV, assigned to the transition between Mn^{3+} ions ($e_g^1 e_g^1 \rightarrow e_g^0 e_g^2$), is accompanied by a minute absorption at lower energies due to some impurities or slight oxygen nonstoichiometry (top panel of Fig. 1). When holes are introduced into this Mott insulator (the PCMO case), the 1.5 eV transition is not identified anymore, and instead absorption at lower energies develops with the charge gap. (The detailed x and T dependences will be discussed later.) For Sr_2MnO_4 without any e_g electron, no sizable absorption is detected below 2 eV. The distinct absorption below 2 eV shown in the mixed valence state of Mn ions has been assigned to the transition from Mn^{3+} to Mn^{4+} ions ($e_g^1 e_g^0 \rightarrow e_g^0 e_g^1$).¹⁶ This idea is supported by the analysis of the electronic spectral weight as measured by the effective number of electrons, $N_{\text{eff}}(\omega_c) = (2m_0/\pi e^2 N) \int_0^{\omega_c} d\omega' \sigma(\omega')$ for $\omega_c = 2$ eV, which is maximized at $x=1/2$ (inset of Fig. 1). Here, according to the Fermi golden rule, the spectral weight of the interband transition should be proportional to the joint density of state. Because in the strong correlation limit the density of states of occupied e_g band in Mn^{3+} and unoccupied e_g band in Mn^{4+} are proportional to $(1-x)$ and x , respectively, the spectral weight of the low energy absorption should follow the functional form of $x(1-x)$.¹⁷ This simple prediction is found to be in good agreement with the doping dependence of N_{eff} for PCMO.¹⁸ It is noted that the spectral feature of the low-energy absorption originating from the electron hopping from Mn^{3+} to Mn^{4+} ions is sensitive to the CO-OO pattern of $\text{Mn}^{3+}/\text{Mn}^{4+}$.

B. Doping-dependent evolution of charge-orbital ordering around half doping

We now turn to the CO-OO state for the PCMO series. At half doping ($x=1/2$), the CO-OO transition occurs at $T_{\text{CO-OO}} \sim 325$ K, which is identified from a sharp increase in the resistivity and a sudden drop in the magnetization curves (Fig. 2). In an electron-diffraction pattern (EDP), superlattice spots are detected below $T_{\text{CO-OO}}$ with a modulation vector $\vec{q} = q\vec{a}^*$ (in the orthorhombic setting), where $q=1/2$ (the bottom panel of Fig. 3). With decreasing x from $1/2$, extra electrons disturb the zigzag e_g orbital arrangement as well as the checkerboard charge ordering. The instability of the charge ordered state is reflected by the gradual suppression of $T_{\text{CO-OO}}$ with decreasing x (top panel of Fig. 3). Finally, no signature of the transition is discerned in resistivity and magnetization curves for $x \leq 0.35$, and superlattice peaks in the EDP turn out to be diffuse, implying short-range correlation. No significant change of q for $x \leq 1/2$ implies the fade-away of the $q=1/2$ CO-OO without any crossover to other types of striped phase. In contrast, it appears that the removal of e_g electrons, i.e., increase of x , does not weaken the stability of the CO-OO. Namely, in the high doping region of $x \geq 1/2$ the $T_{\text{CO-OO}}$ holds in the T range comparable to that for $x=1/2$ (top panel of Fig. 3). According to the EDP mea-

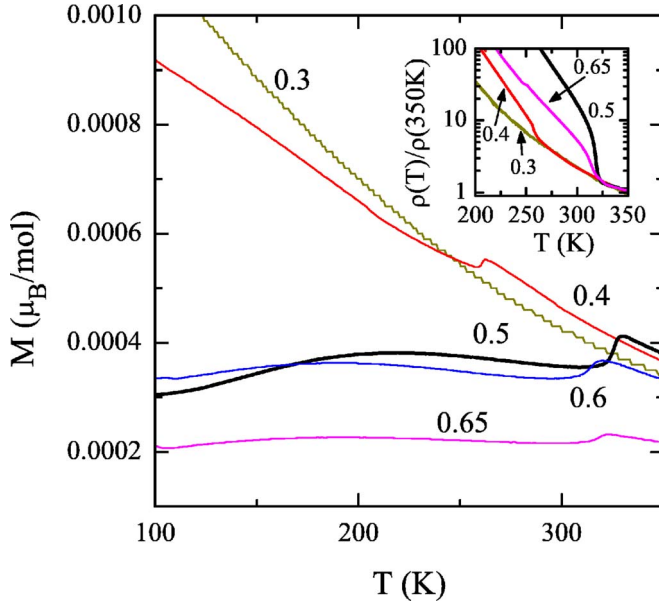


FIG. 2. (Color online) T -dependent magnetization curves $M(T)$ for the PCMO series. The magnetic field \mathbf{H} is applied along the direction normal to the c axis. Inset: dc resistivity curves normalized by the values at 350 K.

surement, the q values for $x \geq 1/2$ are x dependent, following a general relation that $q = (1-x)$ at the lowest T (the bottom panel of Fig. 3). This linear variation of q has been observed in other layered manganites, $\text{La}_{1-x}\text{Sr}_{1+x}\text{MnO}_4$ (Ref. 8) and $\text{Nd}_{1-x}\text{Sr}_{1+x}\text{MnO}_4$,¹² and interpreted with the Wigner crystal model in which equivalent Mn sites are located as far from each other as possible.^{19,20} According to this model, in the $q = 1/3$ ($x = 2/3$) AFM state, Mn^{3+} stripes are separated by two Mn^{4+} stripes. In analogy to the CE-type magnetic order

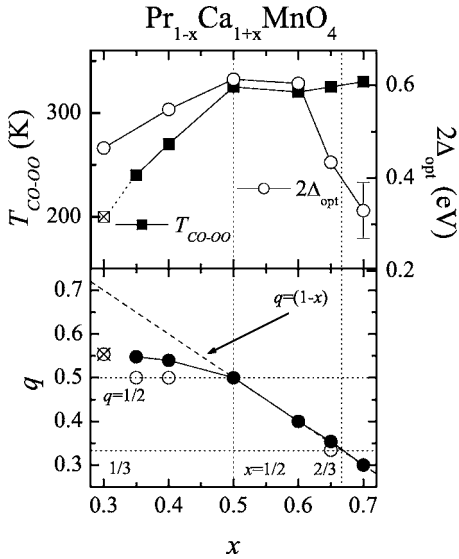


FIG. 3. (Top) T_{CO-OO} , optical gap $2\Delta_{opt}$ at 10 K, and (bottom) modulation vector q for the PCMO series with $0.3 \leq x \leq 0.7$. For $x = 0.3$, the onset temperature of short range of charge ordering T^* is shown. In bottom panel, the solid and the open circles represent q at the lowest T and just below T_{CO-OO} , respectively.

for $x = 1/2$ [Fig. 4(g)], the zigzag FM chains are formed in accord with the e_g orbital ordering, and the chains are coupled antiferromagnetically, as depicted in Fig. 4(h).²⁰⁻²³

C. Correlation between low-energy optical conductivity to charge-orbital ordering pattern

Notably, the optical measurement reveals the variation of the CO-OO state with x . For the $x = 1/2$ CO-OO compound, the absorption near 1 eV exhibits the significant blueshift while sharpening the spectral shape below T_{CO-OO} , which leads to the development of the optical gap $2\Delta_{opt}$ with T [inset of Fig. 4(a)].^{24,25} This behavior is phenomenologically common for various systems with the charge ordering,¹ and the feature for the manganites has been reproduced by some theoretical calculations with the orbital ordering related to the Jahn-Teller distortion.²⁵⁻²⁷ With decreasing x from $1/2$, the low-energy peak is broadened and its T -dependent change as well as the $2\Delta_{opt}$ value are suppressed. These spectral features are suggestive of the weakening of CO-OO. As for the change of the optical response in the high doping region, the spectra for $x = 0.6$ are quite similar to those for $x = 1/2$, whereas for $x \geq 0.65$, the 1 eV absorption shifts to lower energies and its spectral shape is fairly narrow and asymmetric [Fig. 4(e)]. Consequently, the $2\Delta_{opt}$ for $x \geq 0.65$ decreases considerably, even smaller than that for $x = 0.3$. This behavior is rather unexpected in the context of no significant change in T_{CO-OO} for $x \geq 1/2$ (top panel of Fig. 2). We note that the abrupt change of the optical response occurs near $x = 2/3$ ($q = 1/3$). Indeed, the q value for $x = 0.65$ at high T is found to be $1/3$ in close proximity to the $x = 2/3$ state. It is likely that the observed spectral feature near $x = 2/3$ is associated with the specific electronic structure originating from the $q = 1/3$ CO-OO pattern.

D. Theoretical calculation of optical conductivity for $x = 1/3$ and $2/3$

In the following, we try to theoretically understand the peculiar doping dependence of optical response revealed above. In the ground state of the AFM CO-OO state (CE phase), the electron transfer is expected to be confined along the FM zigzag chain. Then, we take the following minimal model for a ferromagnetic zigzag chain in the CE phase:

$$\mathcal{H} = - \sum_{\mathbf{r}, \mathbf{r}'} \sum_{\alpha, \beta=1,2} t_{\mathbf{r}, \mathbf{r}'}^{\alpha, \beta} c_{\mathbf{r}\alpha}^\dagger c_{\mathbf{r}'\beta} + U \sum_{\mathbf{r}} n_{\mathbf{r}1} n_{\mathbf{r}2} + E_{JT} \sum_{\mathbf{r}} [u_{\mathbf{r}}^2 + v_{\mathbf{r}}^2 - 2u_{\mathbf{r}}(n_{\mathbf{r}1} - n_{\mathbf{r}2}) - 2v_{\mathbf{r}}(c_{\mathbf{r}1}^\dagger c_{\mathbf{r}2} + c_{\mathbf{r}2}^\dagger c_{\mathbf{r}1})], \quad (1)$$

which has been adopted to predict the in-plane anisotropy in the half-doped case due to the orbital interference within the zigzag chain.²⁸ Here, $c_{\mathbf{r}\alpha}$ ($c_{\mathbf{r}\alpha}^\dagger$) for the number operator $n_{\mathbf{r}\alpha} = c_{\mathbf{r}\alpha}^\dagger c_{\mathbf{r}\alpha}$ denotes the annihilation (creation) operators of the electron at site \mathbf{r} with the e_g orbital α ($=1$ or 2 for $d_{3z^2-y^2}$ or $d_{x^2-y^2}$, respectively). This Hamiltonian given by Eq. (1) contains the orbital-dependent electron transfer $t_{\mathbf{r}, \mathbf{r}'}^{\alpha, \beta}$ between the adjacent sites \mathbf{r} and \mathbf{r}' with the same spin polarization as the first term and the local interorbital Coulomb and the Jahn-Teller interactions U and E_{JT} as the second and the third terms, respectively. $u_{\mathbf{r}}$ and $v_{\mathbf{r}}$ denote the local Jahn-Teller

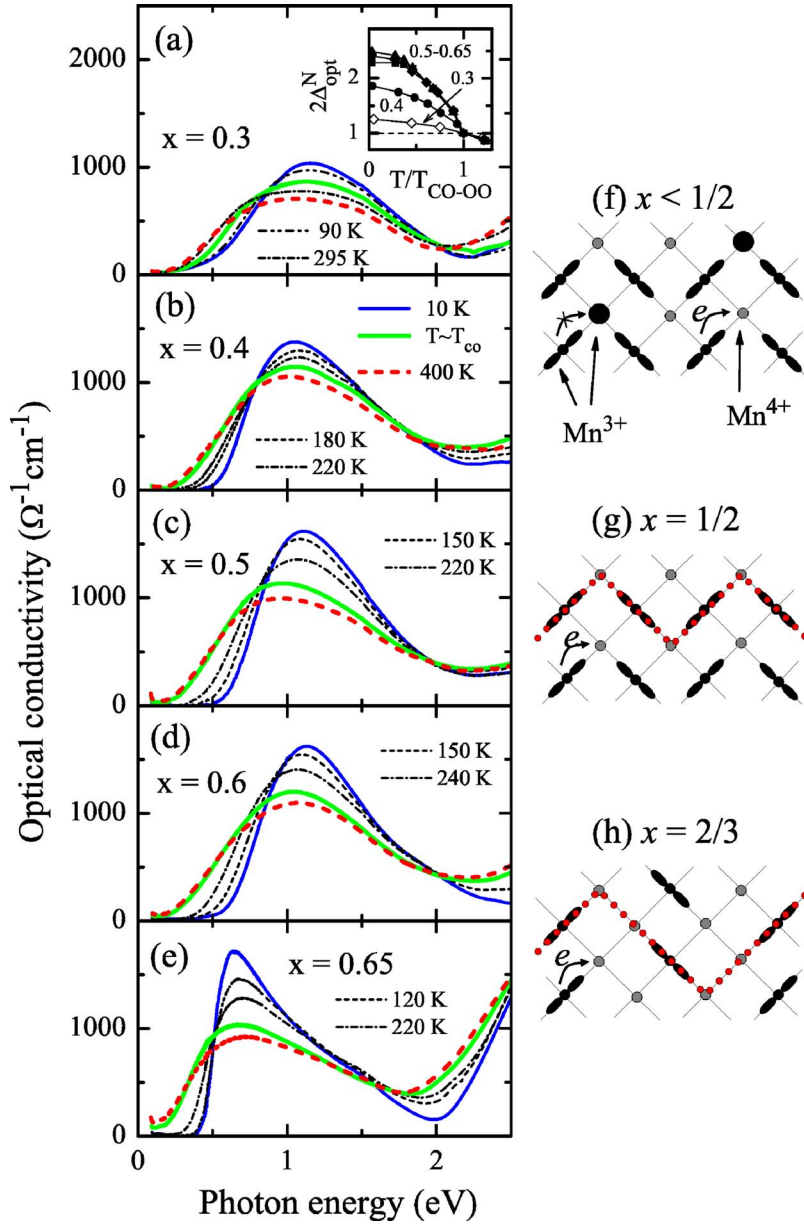


FIG. 4. (Color online) [(a)–(e)] T -dependent $\sigma(\omega)$ for the PCMO series with $x=0.3, 0.4, 0.5, 0.6$, and 0.65 . The thin (blue) solid, the thick (green) solid, and the thick dotted (red) lines represent the 10 K, $T_{\text{CO-OO}}$, and 400 K data, respectively. The inset displays the normalized optical gap $2\Delta_{\text{opt}}^N$ by a value at $T_{\text{CO-OO}}$ (T^* for $x=0.3$) with normalized T by $T_{\text{CO-OO}}$. The $2\Delta_{\text{opt}}^N$ values were estimated from crossing points of abscissa with linear extrapolation of $\sigma(\omega)$. In (f)–(h), schematic diagrams for charge-orbital ordered states are shown at various x . The details are in the text. The arrows indicate the local electron hopping. The dotted line represents a single ferromagnetic zigzag chain.

modes for the MnO_6 octahedron centered at the Mn site \mathbf{r} . We take the Franck-Condon approximation by neglecting the dynamics of these Jahn-Teller modes, which is justified for the strong Jahn-Teller coupling case as in the present situation. As for the orbital and directional dependencies of the transfer integrals, we take the Slater-Koster parameters²⁹ with the electron transfer $V_{dd\sigma} = t \sim 0.25$ eV for the $dd\sigma$ bonding, which is taken as the energy unit.

When this consideration on each zigzag chain is applied to $x=1/2$ and $2/3$ phases, a distinct difference is the number of Mn ions on an elementary straight segment in the zigzag chain structure, i.e., three and four sites for $x=1/2$ and $2/3$, respectively, which yield the periodicities of 4 and 6, respectively. Assuming the periodicity for each case, we solve this model Hamiltonian within the Hartree-Fock approximation to obtain the self-consistent values for $\langle c_{\mathbf{r}\alpha}^\dagger c_{\mathbf{r}'\alpha'} \rangle$ as well as the Jahn-Teller distortions $u_{\mathbf{r}}$ and $v_{\mathbf{r}}$. We note that Hartree-Fock treatment provides a reasonable description of the

ground state even at the large U . For instance, in the case of $x=1/2$, we have obtained the CO-OO pattern characterized by the charge disproportionation δn and the dominant orbital character of $d_{3x^2-y^2}/d_{3y^2-r^2}$ at the electron-rich ($\frac{1+\delta n}{2}$) sites and $d_{x^2-y^2}$ at the electron-poor ($\frac{1-\delta n}{2}$) ones. For this ordering, the Jahn-Teller coupling is indispensable, as previously pointed out,³⁰ and the ground-state properties are insensitive to the choice of U .

In the following, we choose $U=8t$ and $E_{JT}=2t$ to reproduce the experimentally observed optical gap.²⁸ This choice of $E_{JT}=2t$ gives the charge (or orbital) disproportionation; namely, the charge concentrations obtained in the calculation are 0.78 and 0.22 (0.52, 0.32, and 0.16) for two (three) Mn ion sites sharing one electron at $x=1/2$ ($2/3$). It has been known from the first-principles calculation that such charge disproportionation is suppressed by the screening effect and then only the orbital order and the associated Jahn-Teller distortion remain robust.³¹ Using the Hartree-Fock solutions,

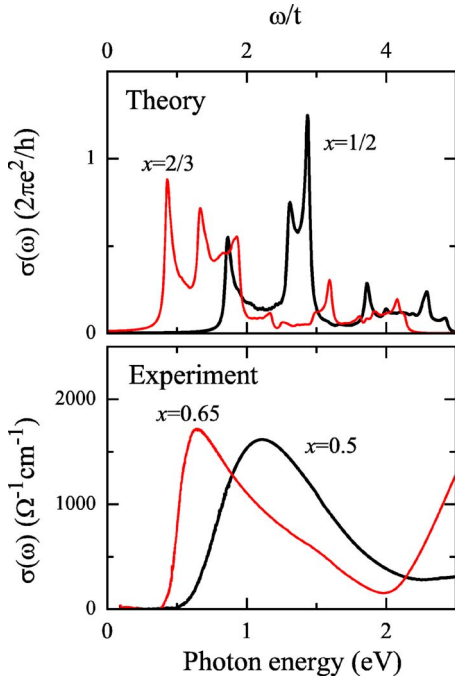


FIG. 5. (Color online) (Top) Calculated $\sigma(\omega)$ for $x=1/2$ and $2/3$ using the Hartree-Fock method. (Bottom) Experimental $\sigma(\omega)$ for $x=0.5$ and 0.65 at 10 K.

we have calculated the in-plane optical conductivity $\sigma(\omega)$. While as in our previous paper,²⁸ the in-plane anisotropy emerges not only for $x=1/2$ but also for $2/3$ between the chain and stripe directions, here, we concentrate on the averaged quantity for comparison with experiments.

Figure 5(a) displays the results of the calculation for each single zigzag ferromagnetic chain at two doping concentrations $x=1/2$ and $2/3$. The calculated optical conductivity for $x=2/3$ exhibits much smaller $2\Delta_{\text{opt}}$ than that for $x=1/2$, with rather asymmetric spectral feature. While the asymmetry of the spectral shape originates from the enhanced 1D character³² with a longer periodicity, the smaller $2\Delta_{\text{opt}}$ reflects the suppression of the charge disproportionation which is equivalent to the local Jahn-Teller distortion. We also performed the calculation for low doping region. Compared with the case for $x \geq 1/2$, the $2\Delta_{\text{opt}}$ for $x < 1/2$ does not change significantly. With adding electrons to the $x=1/2$ state, the local Jahn-Teller distortion is insensitive to doped electrons that occupy mainly electron-poor sites, whereas, for $x \geq 1/2$, it is suppressed by doped holes that go exclusively to electron-rich sites. As far as the CO correlation is concerned, the absorption feature for $x \leq 1/2$ should be similar to that for $x=1/2$, while reducing its spectral weight. It is because extra Mn^{3+} ions [large solid circles in Fig. 4(f)] cannot participate in the electron hopping concerned here due to the local Coulomb energy cost. These theoretical results are in good agreement with our experimental data, as shown in Fig. 5. It can be concluded that the electron hopping along the zigzag chain pathway together with the modulation of the d orbitals and the associated Jahn-Teller distortion plays a

crucial role in the charge dynamics property in the CO-OO state.

E. Role of orbital correlation in the asymmetric doping-dependence of charge-orbital ordering near half-doping

The studies detailed above uncover facets of the role of orbital degree of freedom in the formation of the striped phase. The e_g orbital correlation is responsible for the asymmetric doping dependence in the layered manganite. In the case of perovskite manganites, the competition between FM and CO correlations appears to lead to the asymmetric doping dependence of the modulation vector, which has been recently reproduced phenomenologically using Landau-Ginzburg theory.³³ On the other hand, the FM instability is completely suppressed in the 214 structures and hence cannot be involved in the weakening of the CO-OO with the added e_g electrons from $x=1/2$. Because the $d_{3x^2-r^2} e_g$ orbital accompanies the local Jahn-Teller distortion, the increase of the number of the orbital stripes for $x \leq 1/2$ may require a fairly large energy cost of the lattice strain. The electron-rich striped phase (hole stripe), e.g., the commensurate $x=1/3$ phase ($N[\text{Mn}^{3+}(\text{electron})]:N[\text{Mn}^{4+}(\text{hole})]=2:1$) does not show up, and instead, the $q=1/2$ ($x=1/2$) correlation persists down to a fairly low doping ($x \sim 0.35$) for PCMO. In the high doping range ($x \geq 1/2$), the evolution of charge-orbital striped phase is strongly doping dependent, which is quite analogous to the hole striped phase of Cu and Ni oxides apart from the reverse charge (electron vs hole) distribution. A clear difference in optical response between $x=1/2$ and $\sim 2/3$ is suggestive of a crucial role of the commensurate periodicity in determining a singular electronic structure. In manganites, the electron hopping occurs not along the stripe but along the zigzag chain in accord with the e_g orbital arrangement. A wider spacing between the stripes leads to a longer 1D path for the electron transfer. It has been suggested¹² that at higher doping levels, the CE-type order (antiferromagnetic order of $d_{3x^2-r^2}/3y^2-r^2$, zigzag FM stripe) is changed into the C-type order (ferroic order of $d_{3x^2-r^2}$, straight FM stripe). In this sense, the CO-OO stripe in the manganite provides an ideal laboratory to study the 1D system with controllable nanoscale periodicity and chain configuration.

IV. SUMMARY

We have presented the asymmetric doping-dependent evolution of the charge-orbital ordered state with respect to the addition or removal of e_g electrons from $x=1/2$ for the $\text{Pr}_{1-x}\text{Ca}_{1+x}\text{MnO}_4$ series. The optical response changes dramatically with the stripe periodicity, which is indicative of the crucial role of the nanoscale orbital correlation in determining the electronic structure of the striped manganite.

ACKNOWLEDGMENTS

The authors thank S. Miyasaka for useful discussions. Y.S.L. was supported by the Soongsil University Research Fund.

- ¹M. Imada, A. Fujimori, and Y. Tokura, *Rev. Mod. Phys.* **70**, 1039 (1998).
- ²J. B. Goodenough, *Phys. Rev.* **100**, 564 (1955).
- ³B. J. Sternlieb, J. P. Hill, U. C. Wildgruber, G. M. Luke, B. Nachumi, Y. Moritomo, and Y. Tokura, *Phys. Rev. Lett.* **76**, 2169 (1996).
- ⁴Y. Murakami, H. Kawada, H. Kawata, M. Tanaka, T. Arima, Y. Moritomo, and Y. Tokura, *Phys. Rev. Lett.* **80**, 1932 (1998).
- ⁵Y. Tokura and N. Nagaosa, *Science* **288**, 462 (2000).
- ⁶M. W. Kim, J. H. Jung, K. H. Kim, H. J. Lee, Jaejun Yu, T. W. Noh, and Y. Moritomo, *Phys. Rev. Lett.* **89**, 016403 (2002).
- ⁷Y. Tokura, *Rep. Prog. Phys.* **69**, 797 (2006).
- ⁸S. Larochelle, A. Mehta, L. Lu, P. K. Mang, O. P. Vajk, N. Kaneko, J. W. Lynn, L. Zhou, and M. Greven, *Phys. Rev. B* **71**, 024435 (2005). The neutron scattering results indicate that the ferromagnetic correlation is too weak to detect in the phase diagram of $\text{La}_{1-x}\text{Sr}_{1+x}\text{MnO}_4$.
- ⁹M. Ibarra, R. Retoux, M. Hervieu, C. Autret, A. Maignan, C. Martin, and B. Raveau, *J. Solid State Chem.* **170**, 361 (2003).
- ¹⁰R. Mathieu, J. P. He, X. Z. Yu, Y. Kaneko, M. Uchida, Y. S. Lee, T. Arima, A. Asamitsu, and Y. Tokura, cond-mat/0701191 (to be published).
- ¹¹Y. Moritomo, Y. Tomioka, A. Asamitsu, Y. Tokura, and Y. Matsui, *Phys. Rev. B* **51**, R3297 (1995).
- ¹²T. Kimura, K. Hatsuda, Y. Ueno, R. Kajimoto, H. Mochizuki, H. Yoshizawa, T. Nagai, Y. Matsui, A. Yamazaki, and Y. Tokura, *Phys. Rev. B* **65**, 020407(R) (2001).
- ¹³Y. Moritomo, T. Arima, and Y. Tokura, *J. Phys. Soc. Jpn.* **64**, 4117 (1995).
- ¹⁴J. Matsuno, Y. Okimoto, M. Kawasaki, and Y. Tokura, *Phys. Rev. Lett.* **95**, 176404 (2005).
- ¹⁵An additional weak structure between the second and third peaks for LaSrMnO_4 and Sr_2MnO_4 might be due to the splitting of t_{2g} bands in the layered structure or a transition between t_{2g} bands.
- ¹⁶Y. Okimoto, Y. Tomioka, Y. Onose, Y. Otsuka, and Y. Tokura, *Phys. Rev. B* **57**, R9377 (1998).
- ¹⁷H. Eskes, M. B. J. Meinders, and G. A. Sawatzky, *Phys. Rev. Lett.* **67**, 1035 (1991).
- ¹⁸While the similar relation was reported for pseudocubic perovskite manganites [M. Kim, J. Jung, K. Kim, H. Lee, J. Yu, T. Noh, and Y. Moritomo, *Phys. Rev. Lett.* **89**, 016403 (2002)], the way to estimate the spectral weight is different from that used here in view of the peak assignment and the related spectral range. Kim *et al.* fitted the $\sigma(\omega)$ below 20 eV with two Lorentz oscillators. One at ~ 0.5 eV and the other at ~ 1.5 eV are assigned to be a hopping transition from Mn^{3+} to Mn^{4+} and a transition between Jahn-Teller split e_g orbitals in Mn^{3+} , respectively. They claimed that while the spectral weights of two peaks are rather comparable, that of the former is proportional to a functional form of $x(1-x)$ in the doping range of $0.3 \leq x \leq 0.65$.
- ¹⁹Takashi Hotta, Yasutami Takada, Hiroyasu Koizumi, and Elbio Dagotto, *Phys. Rev. Lett.* **84**, 2477 (2000).
- ²⁰P. G. Radaelli, D. E. Cox, L. Capogna, S.-W. Cheong, and M. Marezio, *Phys. Rev. B* **59**, 14 440 (1999).
- ²¹C. H. Chen, S.-W. Cheong, and H. Y. Hwang, *J. Appl. Phys.* **81**, 4326 (1997).
- ²²J. C. Loudon, S. Cox, A. J. Williams, J. P. Attfield, P. B. Littlewood, P. A. Midgley, and N. D. Mathur, *Phys. Rev. Lett.* **94**, 097202 (2005).
- ²³T. Nagai, T. Kimura, A. Yamazaki, T. Asaka, K. Kimoto, Y. Tokura, and Y. Matsui, *Phys. Rev. B* **65**, 060405(R) (2002).
- ²⁴T. Ishikawa, K. Ookura, and Y. Tokura, *Phys. Rev. B* **59**, 8367 (1999).
- ²⁵J. H. Jung, J. S. Ahn, Jaejun Yu, T. W. Noh, Jinhyoung Lee, Y. Moritomo, I. Solovyev, and K. Terakura, *Phys. Rev. B* **61**, 6902 (2000).
- ²⁶M. Cuoco, C. Noce, and A. M. Oles, *Phys. Rev. B* **66**, 094427 (2002).
- ²⁷J. Bala and P. Horsch, *Phys. Rev. B* **72**, 012404 (2005).
- ²⁸Y. S. Lee, S. Onoda, T. Arima, Y. Tokunaga, J. P. He, Y. Kaneko, N. Nagaosa, and Y. Tokura, *Phys. Rev. Lett.* **97**, 077203 (2006). While the in-plane anisotropy is acquired with respect to the light polarization parallel to the chain or stripe, the averaged spectra are displayed for comparison with experimental results obtained for twinned samples.
- ²⁹W. A. Harrison, *Electronic Structure and the Properties of Solids* (Dover, New York, 1989).
- ³⁰J. Bala, P. Horsch, and Frank Mack, *Phys. Rev. B* **69**, 094415 (2004).
- ³¹P. Mahadevan, K. Terakura, and D. D. Sarma, *Phys. Rev. Lett.* **87**, 066404 (2001).
- ³²Y. S. Lee, J. S. Lee, K. W. Kim, T. W. Noh, Jaejun Yu, E. J. Choi, G. Cao, and J. E. Crow, *Europhys. Lett.* **55**, 280 (2001).
- ³³G. C. Milward, M. J. Calderón, and P. B. Littlewood, *Nature (London)* **433**, 607 (2002).